frontiers in Plant Science

ORIGINAL RESEARCH
published: 26 November 2018
doi: 10.3389/fpls.2018.01739

Elevated CO_2 Improves Photosynthesis Under High Temperature by Attenuating the Functional Limitations to Energy Fluxes, Electron Transport and Redox Homeostasis in Tomato Leaves

Caizhe Pan[1†], Golam Jalal Ahammed[2†], Xin Li[3] and Kai Shi[1]*

[1] Department of Horticulture, Zhejiang University, Hangzhou, China, [2] College of Forestry, Henan University of Science and Technology, Luoyang, China, [3] Tea Research Institute, Chinese Academy of Agricultural Sciences, Hangzhou, China

OPEN ACCESS

Edited by:
Marian Brestic, Slovak University of Agriculture, Slovakia

Reviewed by:
Parvaiz Ahmad, Sri Pratap College Srinagar, India
Basharat Ali, Universität Bonn, Germany

***Correspondence:**
Golam Jalal Ahammed
ahammed@haust.edu.cn

[†]*These authors have contributed equally to this work*

Specialty section:
This article was submitted to Plant Abiotic Stress, a section of the journal Frontiers in Plant Science

Received: *05 August 2018*
Accepted: *08 November 2018*
Published: *26 November 2018*

Citation:
Pan C, Ahammed GJ, Li X and Shi K (2018) Elevated CO_2 Improves Photosynthesis Under High Temperature by Attenuating the Functional Limitations to Energy Fluxes, Electron Transport and Redox Homeostasis in Tomato Leaves. Front. Plant Sci. 9:1739. doi: 10.3389/fpls.2018.01739

Elevated atmospheric CO_2 improves leaf photosynthesis and plant tolerance to heat stress, however, the underlying mechanisms remain unclear. In this study, we exposed tomato plants to elevated CO_2 (800 μmol mol^{-1}) and/or high temperature (42°C for 24 h), and examined a range of photosynthetic and chlorophyll fluorescence parameters as well as cellular redox state to better understand the response of photosystem II (PSII) and PSI to elevated CO_2 and heat stress. The results showed that, while the heat stress drastically decreased the net photosynthetic rate (P_n), maximum carboxylation rate (V_{cmax}), maximum ribulose-1,5-bis-phosphate (RuBP) regeneration rate (J_{max}) and maximal photochemical efficiency of PSII (F_v/F_m), the elevated CO_2 improved those parameters under heat stress and at a 24 h recovery. Furthermore, the heat stress decreased the absorption flux, trapped energy flux, electron transport, energy dissipation per PSII cross section, while the elevated CO_2 had the opposing effects that eventually decreased photoinhibition, damage to photosystems and reactive oxygen species accumulation. Similarly, the elevated CO_2 helped the plants to maintain a reduced redox state as evidenced by the increased ratios of ASA:DHA and GSH:GSSG under heat stress and at recovery. Furthermore, the concentration of $NADP^+$ and ratio of $NADP^+$ to NADPH were induced by elevated CO_2 at recovery. This study unraveled the crucial mechanisms of elevated CO_2-mediated changes in energy fluxes, electron transport and redox homeostasis under heat stress, and shed new light on the responses of tomato plants to combined heat and elevated CO_2.

Keywords: heat stress, elevated CO_2, tomato, chlorophyll fluorescence transient, electron transport, redox

INTRODUCTION

Since the initial era of plant establishment in the terrestrial ecosystem, photosynthesis has been serving as a key process for sustaining any life forms on the earth (Cousins et al., 2014; Brestic et al., 2018). Carbon dioxide (CO_2) is the basic input for the photosynthesis in green plants; however, excess or low CO_2 has diverse effects on plant growth and productivity (Amthor, 1995; Sage and Coleman, 2001). Over the last couple of centuries, the concentration of atmospheric CO_2 has increased tremendously. It is projected that global atmospheric CO_2 concentration will be doubled (800 ppm) by the end of the 21st century (Field et al., 2014). However, due to sessile life style, plants have to endure unfavorable weather events such as high temperature, cold, drought, flood and salinity (Ahuja et al., 2010; Ohama et al., 2017). Elevated atmospheric CO_2 concentrations can not only improve plant growth and productivity, but also enhance plant tolerance to a range of abiotic stresses including high temperature and drought (AbdElgawad et al., 2015; Zinta et al., 2018). However, the mechanisms of plant responses to combined heat and elevated CO_2 remain poorly understood (Cassia et al., 2018; Zhang et al., 2018; Zinta et al., 2018).

Photosynthesis is one of the most temperature-sensitive processes in plants and growth temperature is a key factor as it determines the CO_2 fixation capacity as well as the activity of photosynthetic apparatus (Brestic et al., 2018). Being sessile, most plants inherently possess the ability to adjust their photosynthetic characteristics following a change in their growth temperatures. Heat stress causes dehydration in aerial plant parts, oxidative damage to biomembranes due to increases in reactive oxygen species (ROS) production, decreased growth and a consequent reduction in water use efficiency (Li et al., 2016; Jayawardena et al., 2017). Damage to any component of photosynthesis such as photosynthetic pigments, the two photosystems (PS I & II), electron transport chain, and CO_2 reduction pathways, is sufficient enough to hinder the overall photosynthetic mechanism of a plant (Brestic et al., 2018). Among those key components, photosystem II (PSII) is the most thermosensitive and thus inhibition of photosynthesis may appear before the impairment of other cellular functions following heat stress. Heat stress results in inhibition or inactivation of PSII by degrading the reaction center (RC)-binding protein D1 of PSII (Yoshioka et al., 2006).

Chlorophyll fluorescence measurements have been implicated as non-invasive, rapid and easy to use methods for the evaluation of thermotolerance in plants (Rapacz, 2007; Yan et al., 2013; Li et al., 2016; Brestic et al., 2018). Concerning the chlorophyll fluorescence parameters, most of the studies focused mainly on the maximal photochemical efficiency of PSII (F_v/F_m) (Ahammed et al., 2015; Li et al., 2015), however, the F_v/F_m represents the efficiency that absorbed photons are used for photochemistry (Force et al., 2003; Strasser et al., 2004). Therefore, impairment in energy flow from Q_A due to decreased carboxylation or reduced pool size of acceptors may not affect the F_v/F_m ratio. The JIP-test of the fast fluorescence transient was developed by Strasser and Strasser (1995), which made possible to analyze specific details of changes in energy transfer within the PSII (Yan et al., 2013). These measurement help to establish the relationships between primary photochemistry and the requirement for electrons in later stages of photosynthetic metabolism and can describe the linkage between the biophysical signatures (chlorophyll fluorescence) and the biological functions (Strasser et al., 2004). Previous studies of changes in chlorophyll fluorescence under heat stress have revealed that the imbalance in light absorption and utilization triggers excessive production of ROS that cause damage to photosynthetic apparatus (Li et al., 2016). Particularly, aerial heat stress suppresses photosynthesis mainly by inactivating PSII acceptor side. Despite the stimulatory effect of elevated CO_2 on photosynthesis under heat stress, how energy absorption, distribution, electron transport through PSII and I are influenced in response to elevated CO_2 remains unclear.

Tomatoes (*Solanum lycopersicum* L.) are cultivated as an annual vegetable crop worldwide. Similar to the field-grown tomatoes, greenhouse tomatoes also face challenges from various environmental stressors such as high temperature and salinity as the infrastructures at the farmers' levels are not automated and have no precise temperature control systems in the developing countries like China (Li et al., 2015; Yi et al., 2018). Moreover, boosting crop yield by CO_2 enrichment without sufficient control on the atmospheric temperature often exposes a plant to such unfavorable greenhouse conditions. Previously, we found that elevated CO_2 could alleviate heat stress by modulating antioxidant defense system, which was independent of NPR1-dependent salicylic acid signaling and ABA-dependent process in Arabidopsis and tomato, respectively (Ahammed et al., 2015; Li et al., 2015). However, how elevated CO_2 changes photosynthesis, photochemical efficiency and primary photochemistry in leaves under heat stress remains elusive. In the current study, we evaluated a range of photosynthetic and chlorophyll fluorescence parameters as well as cellular redox state to gain mechanistic insights into the response of PSII and PSI to combined heat and elevated CO_2. The results of this study suggest that elevated CO_2 could alleviate the heat stress-induced functional limitations to photosynthesis in tomato leaves.

MATERIALS AND METHODS

Plant Materials and Growth Conditions

Tomato (*S. lycopersicum* L. cv. Hezuo 903) plants were cultured in the controlled growth chambers having following conditions: 600 μmol m^{-2} s^{-1} photosynthetic photon flux density (PPFD), 14 h photoperiod, 26/22°C (day/night) air temperature and 75% relative humidity. Briefly, one healthy seedling was grown per plastic pots (diameter, 10.5 cm; depth, 17.5 cm) containing a mixture of peat, vermiculite and perlite (6:3:1, v:v:v). Optimum moisture in growth media was maintained by daily watering, while fertilization was done with Hoagland's nutrient solution at 3 day interval. At the four-leaf stage, the seedlings were transferred to controlled environment cabinets (E8 Growth Chamber, Conviron, Winnipeg, MB, Canada), where the atmospheric CO_2 was maintained at either 380 μmol mol^{-1} or 800 μmol mol^{-1}, corresponding to "ambient CO_2" and "elevated CO_2" conditions, respectively. The chambers had

advanced control system to ensure a consistent temperature and gas level throughout the chambers. After an acclimation period of 48 h, half of the seedlings from both CO_2 conditions was challenged with a 24 h heat stress (42°C temperature) and then allowed to recover for 24 h. All gas exchange, chlorophyll fluorescence and biochemical parameters were analyzed after 24 h from the commencement of heat stress and at a 24 h recovery following the heat stress. Treatments were replicated four times, where each replicate represents six seedlings.

Estimation of Photosynthesis and RuBisCO Carboxylation Capacity

Net photosynthetic rate (P_n) was measured on the third fully expanded leaves using an open-flow infrared gas analyzer adapted with light and temperature control systems (Li-COR 6400, Li-COR, Lincoln, NE, United States). To determine RuBisCO carboxylation capacity, leaf net CO_2 assimilation rates (A) in response to CO_2, were measured between 1,600 and 10 μmol m^{-2} s^{-1}. Following method of von Caemmerer and Farquhar (1981), an assimilation versus intercellular CO_2 concentration (A/Ci) curve was measured in which the leaf temperature and PPFD were maintained at 25°C and 600 μmol m^{-2} s^{-1}, respectively. The maximum carboxylation rate of Rubisco (V_{cmax}) and maximum rates of RuBP regeneration (J_{max}) were estimated by fitting a maximum-likelihood regression below and above the inflection of the A/Ci response according to the method described by Ethier and Livingston (2004).

Measurement of Maximal Photochemical Efficiency of PSII, Quantum Yield and Electron Transport in PSI and PSII

Chlorophyll fluorescence parameters such as maximum photochemical efficiency of PSII (F_v/F_m) was measured on the third fully expanded leaves after 30 min of dark adaptation using an imaging pulse amplitude modulated (PAM) fluorimeter (IMAG-MAXI; Heinz Walz, Effeltrich, Germany) as described previously (Li et al., 2015). A simultaneous measurement of quantum yield of PSI [Y(I)] and PSII [Y(II)] in tomato leaves was performed with a Dual-PAM-100 system (Heinz Walz, Effeltrich, Germany) on the measure mode of Fluo+P700 (Pfündel et al., 2008). F_0, the minimum fluorescence, was monitored under a weak light pulse (<0.1 μmol m^{-2} s^{-1}). A saturating pulse (10,000 μmol photons m^{-2} s^{-1}) was then applied to obtain the maximum fluorescence after dark adaptation (F_m). The maximum photochemical efficiency of PSII (F_v/F_m) was calculated using the experimentally determined F_0 and F_m, where Fv was the difference between F_0 and F_m. The $P700^+$ signals (P) could vary between a minimum (P700 fully reduced) and a maximum level (P700 fully oxidized). The maximal photo-oxidizable P700 signal (P_m) was measured through the application of a saturation pulse (10,000 μmol photons m^{-2} s^{-1}) after pre-illumination of far-red light for 10 s. The maximum P700+ signal (Pm') was determined similar to P_m but with actinic light instead of far-red light. The slow induction curve was recorded for 300 s to achieve the steady state of the photosynthetic apparatus, and then the actinic light was turned off. After the final saturating pulse, values of effective quantum yield of PSII, Y(II); electron transport rate in PSII, ETR(II), non-photochemical quenching, Y(NPQ); non-regulated non-photochemical energy loss in PSII (non-regulated energy dissipation at PSII centers), Y(NO); effective quantum yield of PSI, Y(I), electron transport rate in PSI, ETR(I); non-photochemical energy dissipation in PSI due to acceptor side limitation (acceptor-limited quenching), Y(NA); and non-photochemical energy dissipation in PSI due to donor side limitation (donor-limited quenching), Y(ND) were recorded for analysis of PSI and PSII activity. The chlorophyll fluorescence parameters were calculated as follows: Fv/Fm = (Fm-Fo)/Fm; Y(II) = (Fm'-Fs)/Fm'; NPQ = (Fm-Fm')/Fm'; Y(I) = (Pm'-P)/Pm; Y(ND) = P/Pm; Y(NA) = (Pm-Pm')/Pm. The relationship of quantum yield of PSI is: Y(I)+Y(ND)+Y(NA) = 1 (Klughammer and Schreiber, 2008; Pfündel et al., 2008). Photosynthetic electron flow through PSI and PSII were calculated as: ETRII = Y(II) × PPFD × 0.84 × 0.5 (Krall and Edwards, 1992), ETRI = Y(I) × PPFD × 0.84 × 0.5 (Yamori et al., 2011), where 0.5 is assumed to be the proportion of absorbed light reaching PSI or PSII, and 0.84 is assumed to be the absorptance (the fraction of the incident light absorbed by leaves).

Histochemical Detection of H_2O_2 and $O_2^{\bullet-}$ Accumulation

Accumulation of H_2O_2 and $O_2^{\bullet-}$ in leaves was visually detected by staining with 3,3-diaminobenzidine (DAB) following method of Thordal-Christensen et al. (1997). Freshly detached leaves were submerged in 1 mg mL^{-1} solution of DAB (pH 3.8) and incubated for 6 h at 25°C. Leaves were then bleached with boiling ethanol (96%, v/v). Bleaching washed out the pigments of leaves except for the deep brown polymerized product of DAB and H_2O_2 reaction. Ascorbic acid was used as antioxidant to confirm that brown spots correspond to H_2O_2 formation. DAB stained leaves were observed and photographed with a light microscopy system (Leica DM4000B & DFC425, Leica micro-system Ltd., Heerbrugg, Germany). $O_2^{\bullet-}$ accumulation in leaves was visualized according to Jabs et al. (1996) through the incubation of leaves in *p*-Nitro-Blue Tetrazolium chloride NBT (0.5 mg mL^{-1}, pH 7.8) solution in dark.

Polyphasic Fluorescence Transients and JIP-Test Parameters

Tomato leaves were dark adapted for 15 min. Then, chlorophyll fluorescence transients were recorded up to 1 s on a logarithmic timescale with a Dual-PAM-100 system (Heinz Walz, Germany). Data were obtained every 20 μs. The polyphasic fluorescence induction kinetics was analyzed according to the JIP test (Strasser and Govindjee, 1992). Initial fluorescence (F_0) was measured at 20 μs using the fast-rise kinetic curves when all PSII RCs are open. $F_{300\mu s}$ is the fluorescence at 300 μs; F_J and F_I are the fluorescence intensity at step J (2 ms) and at step I (30 ms), respectively. The maximal fluorescence (F_m) is the peak of fluorescence at the step P when all RCs are closed. Area is total complementary area between fluorescence induction

curves. As described by Strasser and Strasser (1995) and Strasser et al. (2004), parameters quantifying the PSII behavior, such as absorption flux (ABS), trapped energy flux (TR), electron transport flux (ET), dissipated energy flux (D), and density of PSII RC per excited cross section (at $t = t_{Fm}$, CS_m) were calculated from the above original data as follows:

$$ABS/CS_m \approx F_m$$

$$TR/CS_m = [1 - (F_0/F_m)]^* \left(ABS/CS_m\right)$$

$$ET/CS_m = [1 - (F_0/F_m)]^* \left[1 - \left(F_j - F_0\right) / \left(F_m - F_0\right)\right]^* \left(ABS/CS_m\right)$$

$$D/CS_m = \left(ABS/CS_m\right) - \left(TR/CS_m\right)$$

$$RC/CS_m = [1 - (F_0/F_m)]^* \left[\left(F_j - F_0\right) / \left(F_m - F_0\right)\right]^* \left(ABS/CS_m\right) / \left[4\left(F_{300\ \mu s} - F_0\right) / \left(F_m - F_0\right)\right]$$

Assay of NADPH and $NADP^+$

For the extraction of NADPH and $NADP^+$, 0.3 g fresh leaf tissues were directly homogenized with either 3.0 mL of 0.2 M NaOH or 3.0 mL of 0.2 M HCL, respectively (Zhao et al., 1987). Each homogenate was made to 10 mL with respective NaOH or HCL solution and heated for 5 min in a boiling water bath followed by cooling in an ice bath. Samples were then centrifuged at 10,000 × *g* at 4°C for 10 min. Supernatants were transferred to separate tubes and kept on ice for coenzyme assay.

Enzyme cycling assays of NADPH and $NADP^+$ were performed in low light with MTT as the terminal electron acceptor. Briefly, 50 μL sample supernatant was added to 500 μL mixture containing 0.1 M Tricine-NaOH buffer (pH 8.0), 10 mM EDTA (disodium salt), 1 mM MTT, 2 mM phenazine ethosulfate (PES) and 5 mM G6P, and incubated for 5 min at 37°C. Enzyme cycling was initiated by adding 2 U G6PDH solution and the reaction was stopped by adding 500 μL of 6 M NaCl. Each sample was assayed at 30°C for 30 min. With each biological sample, a blank measurement was also made by adding 0.1 M Tricine-NaOH buffer instead of enzyme. Absorbance was recorded at 570 nm. The rate of reduction of MTT at 570 nm is directly proportional to the concentration of NADPH or $NADP^+$ (Zhao et al., 1987).

Measurement of Ascorbate-Glutathione Pool

Tomato leaf tissue (0.3 g) was homogenized in 2 mL 6% metaphosphoric acid containing 2 mM EDTA and centrifuged at 4°C for 10 min at 12,000 × *g*. The supernatants were used for the determination of ascorbate (AsA), dehydroascorbate (DHA), reduced glutathione (GSH) and oxidized glutathione (GSSG). The AsA and DHA contents were assayed following method of Law et al. (1983) as described elsewhere (Li et al., 2015). The GSH concentration was measured by subtracting the GSSG concentration from the total glutathione concentration according to Rao et al. (1995) by an enzymatic recycling method. All of the spectrophotometric analyses were performed using the Multimode Plate Reader Label-free System (PerkinElmer, Wellesley, MA, United States).

Statistical Analysis

The data were expressed as means ± SD. Statistical analysis was performed using analysis of variance (ANOVA) followed by the Tukey's test to compare significant treatment differences at $P < 0.05$. At least four independent replicates were conducted for each determination.

RESULTS

Elevated CO_2 Improves Photosynthesis, RuBisCO Carboxylation and Regeneration Capacity Under Heat Stress in Tomato

To understand the photosynthetic response of tomato plants to elevated CO_2 and/or heat treatments, we first measured the net photosynthetic rate (P_n) both under heat stress and at recovery. The results showed that heat stress drastically decreased the P_n by 57% and it was not fully restored to the control level at recovery (**Figure 1**). On the contrary, elevated CO_2 exhibited a profound stimulatory effect on the P_n with or without heat stress. Under normal temperature conditions, elevated CO_2 increased the P_n by 45%, while under heat stress and at recovery, elevated CO_2 increased the P_n by 116 and 96%, respectively. Similarly, heat stress decreased the V_{cmax} and J_{max} by 41% compared with that under normal temperature conditions (**Figure 1**). Although V_{cmax} but not J_{max} remarkably increased at recovery, it was still significantly lower than that of control. By contrast, combined heat stress and elevated CO_2 significantly increased the V_{cmax} and J_{max} both under heat stress and at recovery compared with that of ambient CO_2.

Elevated CO_2 Protects PSII Capacity by Lowering ROS Accumulation in Tomato Leaves

As shown in **Figure 2**, heat stress significantly decreased the F_v/F_m by 58%, which was slightly increased after a 24 h recovery period but still remained below the level of control. On the other hand, elevated CO_2 increased the F_v/F_m by 60 and 14% under heat stress and at recovery compared with only heat stress and recovery treatments, respectively. Notably, elevated CO_2 had no effect on the F_v/F_m under normal temperature conditions. To explore whether elevated CO_2-induced heat stress mitigation was associated with the reduced ROS accumulation, we histochemically detected $O_2^{\bullet-}$ and H_2O_2 accumulation in tomato leaves. As expected, $O_2^{\bullet-}$ and H_2O_2 accumulation increased under heat stress, which was slightly attenuated at recovery. However, based on the NBT and DAB staining, elevated CO_2 clearly decreased $O_2^{\bullet-}$ and H_2O_2 accumulation both under heat stress and at recovery (**Figure 2**), indicating that elevated CO_2 protected PSII by reducing the heat stress-induced ROS accumulation.

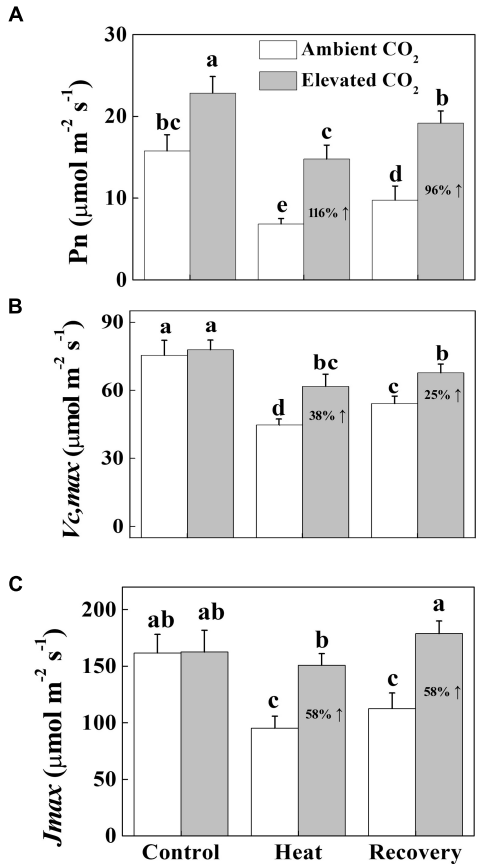

FIGURE 1 | Effects of elevated CO_2 and heat stress either alone or combined on the CO_2 assimilation capacity in tomato leaves. **(A)** the net photosynthetic rate (P_n); **(B)** the maximum carboxylation rate of RuBisCO (V_{cmax}), **(C)** the maximum rate of RuBP regeneration (J_{max}). At the four-leaf stage, tomato seedlings were exposed to either ambient (380 μmol mol^{-1}) or elevated CO_2 concentration (800 μmol mol^{-1}). After an acclimation period of 48 h, half of the seedlings from both CO_2 conditions was challenged with a 24 h heat stress (42°C temperature) and then allowed to recover for 24 h. Measurements were taken on the third fully expanded leaves using an open-flow infrared gas analyzer adapted with light and temperature control systems (Li-COR 6400, Li-COR, Lincoln, NE, United States). The results are expressed as the mean values ± SD, $n = 6$. Different letters above the bars indicate significant differences at $P < 0.05$ according to Tukey's test.

Elevated CO_2 Modulates Photochemical Reactions Under Heat Stress in Tomato Plants

To further elucidate how elevated CO_2 and/or heat stress altered PSII activity, we constructed the leaf models of phenomenological energy fluxes (**Figure 3**) per cross section by using the following parameters: the absorption flux per cross section (ABS/CSm), the trapped energy flux per PSII cross section (TR/CSm), the electron transport in PSII cross section (ET/CSm), the energy dissipation per PSII cross section (D/CSm) and the density of active RCs/CSm. The phenomenological pipeline models of energy fluxes showed that heat stress significantly decreased ABS/CSm, TR/CSm, E/CSm and D/CSm by 34, 36, 36 and 11%, respectively (**Figure 3**). The decreases in those parameters were slightly attenuated at the recovery, however, combined heat stress and elevated CO_2 significantly improved ABS/CSm, TR/CSm and E/CSm by 27, 22 and 41%, respectively, compared with that under only heat stress. The elevated CO_2-induced stimulation on those parameters was also noticeable after the recovery period. For instance, at recovery, the D/CSm under elevated CO_2 increased to the level of only elevated CO_2, which potentially facilitated the dissipation of excess light energy. In addition, the density of active RCs, as indicated by the number of open circles, was also reduced by the heat stress; however, the elevated CO_2 slightly decreased the inactive RC density, as indicated by the number of closed circles, both under heat stress and at recovery (**Figure 3**).

Next, we evaluated some other photochemical reaction-related parameters of the PSI and PSII. Consistent with the changes in F_v/F_m, heat stress decreased Y(II) and Y(I) by 56 and 51%, respectively, compared with that of control (**Figure 4**). In addition, electron transport driven by PSII and PSI significantly decreased by 55 and 50%, respectively, under the heat stress compared with that of the control. While a portion of the absorbed light energy is used for photosynthesis, i.e., photochemistry, the rest is dissipated in the form of heat to minimize excess energy-induced damage to photosynthetic apparatus. Furthermore, heat stress significantly increased the extent of damage to PSII and PSI as evidenced by the increased values of Y(NO) in PSII and Y(NA) in PSI (**Figure 4**). However, at recovery, elevated CO_2 significantly reduced the heat-induced damage to PSII and PSI as evidenced by decreased Y(NO) and Y(NA) values. The dissipation related to light protection capacity of plants, which is represented by the Y(NPQ) in PSII and Y(ND) in PSI, increased significantly by 106 and 116%, respectively, under the heat stress. However, elevated CO_2 significantly decreased the heat-induced increase in Y(ND).

Effects of Elevated CO_2 and/or Heat Stress on the Acceptor Side in Electron Transport Chain

Next, we biochemically analyzed the oxidized nicotin amide adenine ($NADP^+$) concentration, which is the terminal electron acceptor, in the electron transport chain. As shown in **Figure 5**, under heat stress, $NADP^+$ was at the level of control; however, at recovery, $NADP^+$ significantly decreased. Interestingly, neither $NADP^+$ was increased by the elevated CO_2, nor the NADPH was altered by heat and/or elevated CO_2. Similar to the trend of $NADP^+$, the ratio of $NADP^+$ to NADPH decreased only at recovery, which was reversed by the combined heat and elevated CO_2.

Elevated CO_2 Improves Redox Homeostasis in Tomato Leaves Under Heat Stress

ASA-GSH pool plays a critical role in redox homeostasis in plants. Heat stress significantly decreased total ascorbate (ASA+DHA) concentration but increased the ratio of ASA to DHA (ASA/DHA) by 18 and 63%, respectively, compared with that of control (**Figure 6**). These effects of heat stress

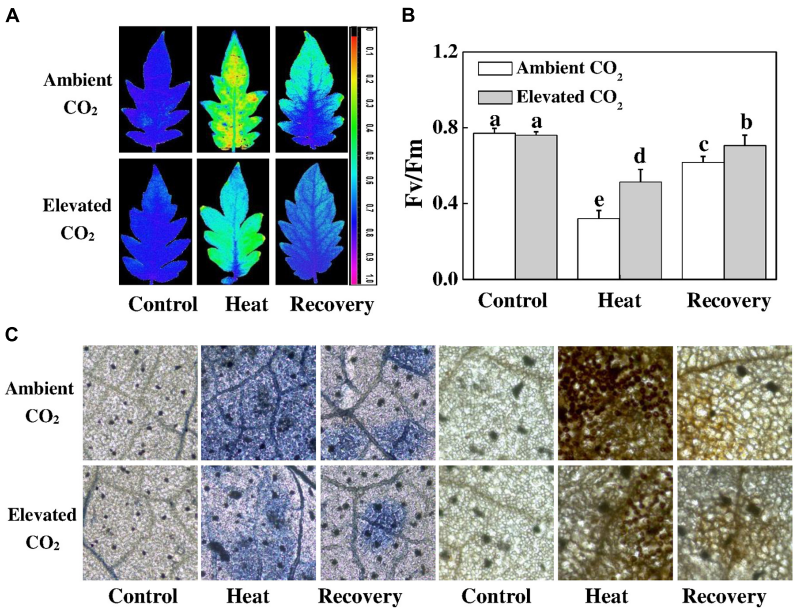

FIGURE 2 | Effects of elevated CO_2 and heat stress either alone or combined on the photosynthetic apparatus and reactive oxygen species accumulation in tomato leaves. **(A)** the maximum photochemical efficiency of photosystem II (F_v/F_m) shown in pseudo color images, the false color code depicted in the image ranges from 0 (black) to 1 (purple); **(B)** F_v/F_m values; and **(C)** *in situ* accumulation of superoxide ($O_2^{\bullet-}$) and hydrogen peroxide (H_2O_2) by NBT and DAB staining in tomato leaves. Tomato seedlings kept at ambient (380 μmol mol^{-1}) and elevated CO_2 concentration (800 μmol mol^{-1}) were challenged with a 24 h heat stress (42°C temperature) and then allowed to recover for 24 h. F_v/F_m was measured on the third fully expanded leaves after 30 min of dark adaptation using an imaging pulse amplitude modulated (PAM) fluorimeter (IMAG-MAXI; Heinz Walz, Effeltrich, Germany). The results are expressed as the mean values ± SD, $n = 6$. Different letters above the bars in **(B)** indicate significant differences at $P < 0.05$ according to Tukey's test.

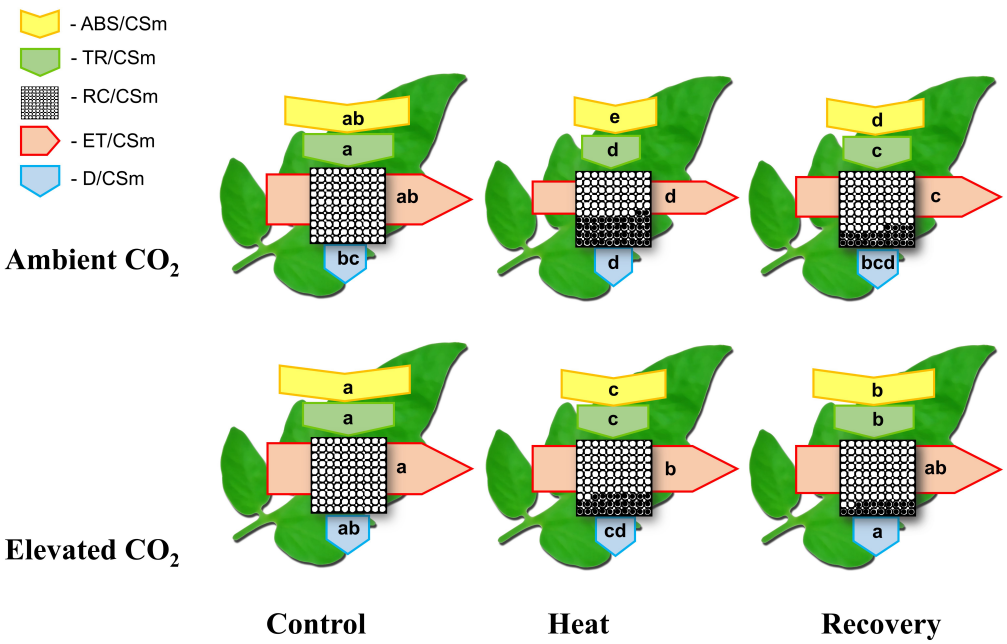

FIGURE 3 | Energy pipeline leaf model of phenomenological fluxes (per cross section, CS) in the third fully expanded leaf in tomato as influenced by elevated CO_2 and heat stress. The results are expressed as the mean values ± SD, $n = 6$. Each relative value is drawn by the width of the corresponding arrow, standing for a parameter. Different letters within the same color arrows indicate significant differences at $P < 0.05$ according to Tukey's test. Empty and full black circles indicate, respectively, the percentage of active (QA reducing) and non-active (non-QA reducing) reaction centers of photosystem II (PSII); ABS/CSm, the absorption flux per cross section; TR/CSm, the trapped energy flux per PSII cross section; ET/CSm, the electron transport in PSII cross section; D/CSm, the energy dissipation per PSII cross section; and RC/CSm, the density of active reaction centers.

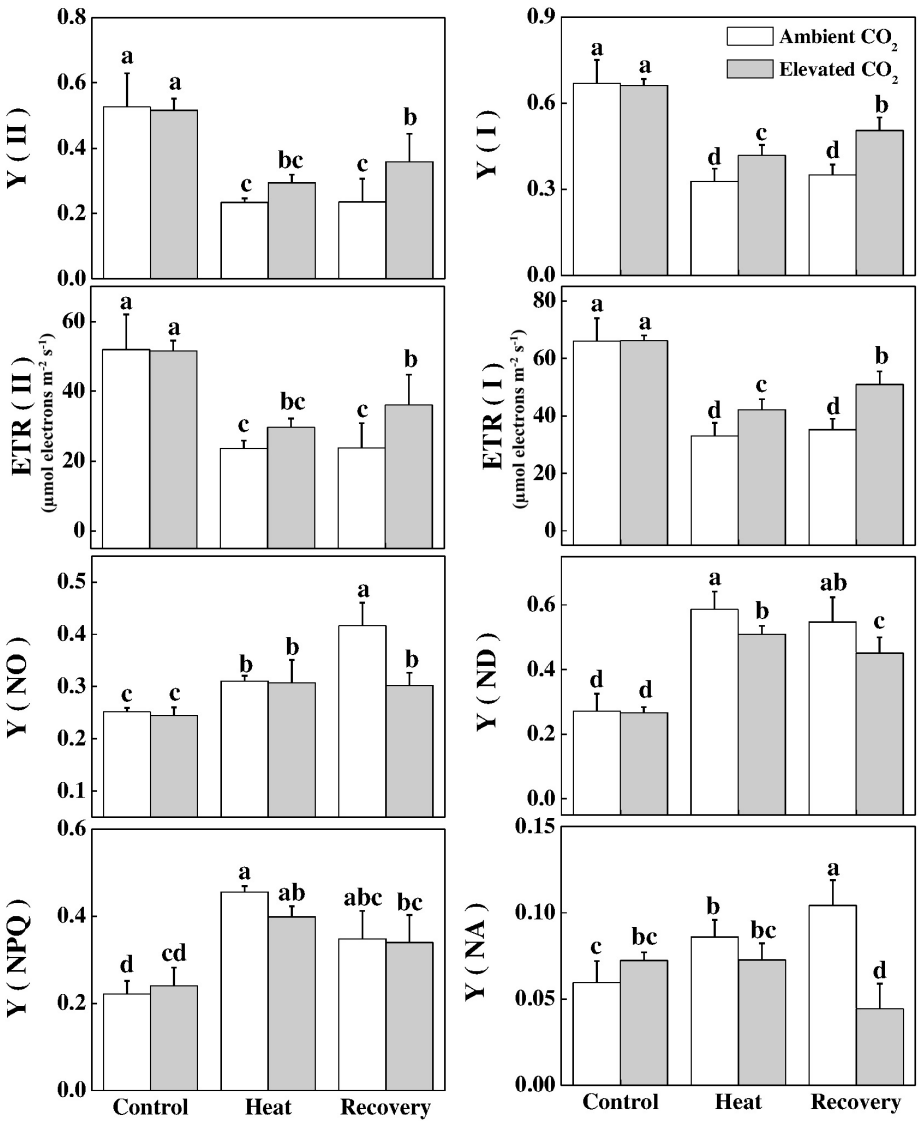

FIGURE 4 | Effects of elevated CO_2 and heat stress either alone or combined on different chlorophyll fluorescence parameters in tomato plants. Tomato seedlings kept at ambient (380 μmol mol^{-1}) and elevated CO_2 concentration (800 μmol mol^{-1}) were challenged with a 24 h heat stress (42°C temperature) and then allowed to recover for 24 h. The bars (means ± SD, $n = 6$) labeled with different letters are significantly different at $P < 0.05$ according to Tukey's test. The effective quantum yield of PSII, Y(II); electron transport rate in PSII, ETR(II), non-photochemical quenching, Y(NPQ); non-regulated non-photochemical energy loss in PSII (non-regulated energy dissipation at PSII centers), Y(NO); effective quantum yield of PSI, Y(I), electron transport rate in PSI, ETR(I); non-photochemical energy dissipation in PSI due to acceptor side limitation (acceptor-limited quenching), Y(NA); and non-photochemical energy dissipation in PSI due to donor side limitation (donor-limited quenching), Y(ND).

on the ASA pool persisted even after the recovery period and the elevated CO_2 treatment had no additional effect on ASA+DHA concentration. However, elevated CO_2 treatment on heat-stressed plants further increased the ASA/DHA ratio by 32% compared with the only heat stress. Furthermore, heat stress increased the ratio of GSH to GSSG (GSG/GSSG) without altering the total glutathione concentration (GSH+GSSG). Elevated CO_2 treatment further increased the GSH/GSSG ratio by 45 and 31% under the heat stress and at recovery, respectively, compared with their respective only treatment without elevated CO_2. All these results indicate that elevated CO_2 helped the plants to maintain a reduced redox state as evidenced by the increased ASA/DHA and GSH/GSSG values under combined heat stress and elevated CO_2.

DISCUSSION

Rising temperature and elevated CO_2 differentially affect plant photosynthetic process (Xu et al., 2015). Heat stress-induced reductions in the photosynthetic capacity due to suppression of RuBisCO activity and RuBP regeneration capacity result in

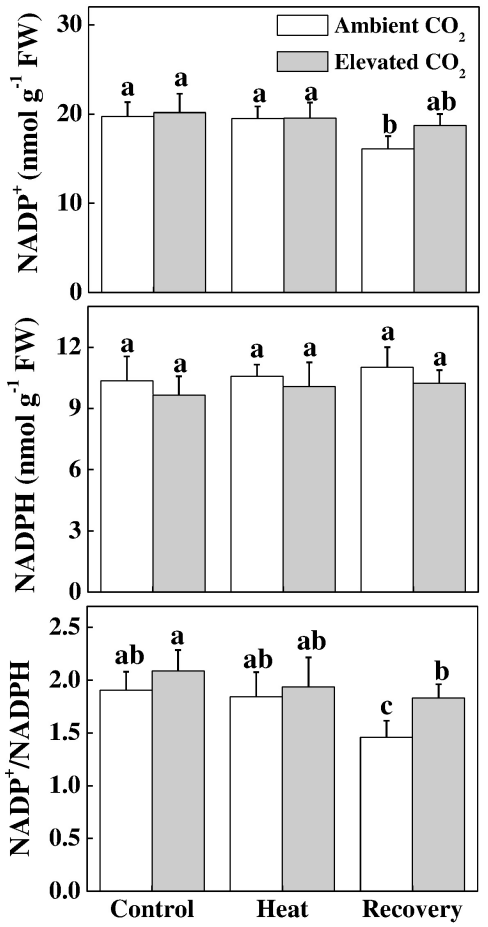

FIGURE 5 | Effects of elevated CO_2 and heat stress either alone or combined on the electron acceptor site in tomato leaves. NADP(H) concentrations were assayed after 24 h heat treatment and at 24 h recovery after the heat stress. Data are the means of four replicates (±SD). Mean denoted by different letters indicate significant differences between the treatments ($P < 0.05$).

reduced consumption of energy equivalent (ATP, NADPH) in the Calvin cycle and thus can increase demand for excess energy dissipation and alternative electron sinks (Lawlor and Tezara, 2009; Ohama et al., 2017). In the current study, we found that heat stress-caused drastic reduction in CO_2 assimilation rate was attributed to simultaneous declines in V_{cmax} and J_{max} (**Figure 1**). Furthermore, heat-induced excessive production of ROS caused damage to photosynthetic apparatus as evidenced by decreased F_v/F_m, low electron transport rate and altered oxidized and reduced states of PSII and PSI (**Figures 2–4**). On the other hand, elevated CO_2 remarkably attenuated heat-induced damage to photosynthetic apparatus and promoted electron transport in PSII and PSI by maintaining proper redox balance (**Figure 6**).

Previous studies have shown that elevated CO_2 can alleviate stress-induced reduction in photosynthetic rate (Cassia et al., 2018). In the current study, we mainly focused on the non-stomatal factors to explore whether and how elevated CO_2 alters intrinsic photosynthetic capacity and energy conversion. We found that elevated CO_2-induced increase in the net photosynthetic rate (P_n) was accompanied with the simultaneous increases in V_{cmax} and J_{max} (**Figure 1**), indicating that increased carbon fixation capacity under elevated CO_2 was partly attributed to increased RuBisCO carboxylation efficiency and RuBP regeneration capacity. It is to be noted that elevated CO_2 decreases allocation of electron transport to photorespiration and increases the electron flow to RuBisCO carboxylation (Robredo et al., 2010). Such mechanisms potentially functioned in the current study, which resulted in the promotion of photosynthesis. While majority of the relevant studies often used F_v/F_m, which is just one of a number of chlorophyll fluorescence parameters (Force et al., 2003), we used fluorescence transient, particularly, the JIP-test that quantified the stepwise flow of energy through PSII (Strasser and Strasser, 1995). This simplified model of the energy fluxes defines energy into an absorbed flux (ABS), a trapping flux (TR, the flux channeled to the RC reducing Q_A to Q_A^-), an electron transport flux (ET, the flux transported beyond Q_A^- which is re-oxidized to Q_A) and a flux of non-trapped energy that is dissipated as heat and some fluorescence (D). As shown in the energy pipeline models (**Figure 3**), heat stress sharply decreased the ABS, TR, ET and D per cross section. However, elevated CO_2 increased those parameters particularly at the recovery.

In the current study, heat-induced reduction in the Y(II) values were primarily due to higher regulated non-photochemical energy dissipation, as reflected by the increased Y(NPQ) values compared with that in the control. However, the higher Y(NO) at recovery compared to that under heat stress potentially indicates an adaptation response since the F_v/F_m increased and ROS accumulation decreased at recovery compared to that under heat stress (**Figures 2**, **4**). Meanwhile, elevated CO_2 decreased quantum yield of non-light-induced non-photochemical fluorescence quenching, i.e., Y (NO) caused by higher fraction of closed PSII centers, leading to a significantly increased Y(II) value compared with that in ambient CO_2 (**Figure 4**). However, Y(NPQ) was not altered by elevated CO_2, implying that elevated CO_2-induced increased P_n serves as a major sink for ATP and NADPH that potentially lowered the necessity for thermal dissipation of energy (**Figure 4**).

Furthermore, we found that the photochemical yield of PS I, Y(I), was slightly higher than that of PSII regardless of heat stress and/or CO_2 conditions. The low Y(I) value in heat-stressed leaves was attributed to both donor and acceptor side limitation of PS I, as evidenced by significantly increased Y(ND) and Y(NA), respectively (**Figure 4**). Our results are in agreement with Li et al. (2016), who inferred that heat stress affected PSII at both donor and acceptor sides and thus limiting photosynthesis. It also reflects that heat stress altered the balance of PSI between reduced and oxidized states. While elevated CO_2 mainly alleviated donor side limitation under the heat stress, it markedly reduced acceptor side limitation at recovery, as reflected by the decreased Y(NA) value compared with ambient CO_2 conditions (**Figure 4**). The increased Y(NA) levels following heat at ambient CO_2 conditions suggest that P700 was potentially over-oxidized which promoted the generation of ROS and caused damage

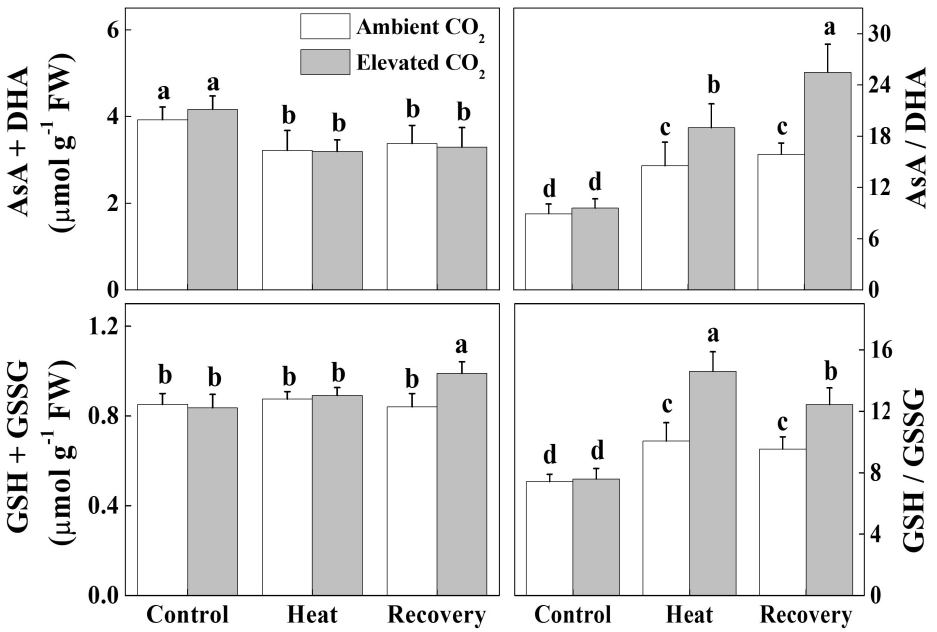

FIGURE 6 | Effects of elevated CO_2 and heat stress either alone or combined on the ascorbate-glutatione (AsA-GSH) pool and redox state in tomato leaves. Leaf samples for biochemical analysis were harvested after 24 h heat treatment and at 24 h recovery after the heat stress along with the control. Data are the means of four replicates (±SD). Mean denoted by different letters indicate significant differences between the treatments ($P < 0.05$). Ascorbate, AsA; dehydro ascorbate, DHA; GSH, reduced glutathione; GSSG, oxidized glutathione.

to the photosynthetic apparatus (Rapacz, 2007). However, ROS accumulation at recovery was lower than that under heat stress, suggesting that ROS scavenging mechanism effectively functioned to minimize ROS level at recovery (**Figure 2**). In addition, increased Y(ND) potentially stimulated the cyclic electron flow (CEF), an alternative electron sink, and its enhancement would decrease the energetic pressure and ROS formation during photochemical reactions (Zhang et al., 2015; Wang et al., 2018). CEF around PSI is believed to affect NAD(P)H dehydrogenase complex-dependent pathways and suppression of CEF inhibits the D1 protein synthesis and enhances photoinhibition (Yoshioka et al., 2006; Takahashi and Murata, 2008). This implies that elevated CO_2 can promote PS I photochemistry by alleviating the limitations in both donor and acceptor sides.

The oxidized nicotin amide adenine ($NADP^+$) is the terminal electron acceptor of the linear electron transport chain that receives electron to generate NADPH to be consumed in Calvin cycle for CO_2 fixation (Farquhar et al., 1980; Strasser et al., 2004; Raines, 2011). In our experiments, heat stress decreased the ratio of $NADP^+$/NADPH at recovery (**Figure 5**), which potentially suppressed Calvin cycle capacity by inhibiting the activation state and activity of RuBisCO, leading to the reduced rate of $NADP^+$ regeneration (Li et al., 2016). It is well known that heat stress-induced reduction in RuBisCO activity is associated with decreased stomatal conductance that limits CO_2 supply and causes photo-damage to PSII via excessive reduction of Q_A. Meanwhile, heat stress not only inhibits the synthesis of D1 protein in the PSII RC, but also impedes the repair of PSII (Takahashi and Murata, 2008). Heat-induced excessive production of ROS could suppress synthesis of D1 protein, which eventually decreases PSII activity and causes imbalance between the generation and utilization of electrons, leading to photoinhibition (Li et al., 2015, 2016). We may argue that heat-induced excessive production of ROS potentially blocked the electron transport, disrupted redox balance and affected the repair process of PSII (Yan et al., 2013; Brestic et al., 2018). However, elevated CO_2 maintained a similar ratio of $NADP^+$/NADPH at recovery as of control (**Figure 5**) which potentially stimulated electron transport and the utilization of light-sourced chemical energy in the Calvin cycle (Yan et al., 2013; Brestic et al., 2018). The redox poise in photosystems is dependent on multiple factors and maintenance of high ratios of GSH/GSSG and AsA/DHA are crucial for plant tolerance to high temperature (Foyer, 2018; Kaur et al., 2018). The analysis of ascorbate and glutathione redox state reveals that elevated CO_2 maintained a reduced redox state both under heat stress and at recovery (**Figure 6**), which might minimize ROS generation and keep balance between electron generation and utilization (**Figures 2**, **5**). This homeostasis makes intuitive sense because the products of linear electron transport, ATP and NADPH, are utilized directly in photosynthetic carbon assimilation in Calvin Cycle in a known ratio, in which one molecule of glucose is produced from 6 CO_2, 18 ATP and 12 NADPH (Raines, 2011).

In summary, we found that heat stress drastically decreased the net photosynthetic rate (P_n), maximum

carboxylation rate (V_{cmax}), maximum RuBP regeneration rate (J_{max}) and maximal photochemical efficiency of PSII (F_v/F_m) in tomato leaves. However, elevated CO_2 improved those parameters both under heat stress and at recovery. Heat stress also decreased the absorption flux, trapped energy flux, electron transport and energy dissipation per PSII cross section, whereas elevated CO_2 alleviated photoinhibition, damage to photosystems and ROS accumulation. Plants grown at elevated CO_2 maintained a reduced redox state as evidenced by the increased ASA:DHA and GSH:GSSG ratios under the heat stress. Our results shed some light on the mechanisms of plant responses to combined heat stress and elevated CO_2, and might be useful to exploring proper management strategies for greenhouse vegetable production.

AUTHOR CONTRIBUTIONS

KS, GA, and XL planned the research. CP, GA, and XL performed the experiments. GA, XL, and KS analyzed and discussed the data. GA wrote the article with contribution from the other authors.

FUNDING

This study was funded by the National Natural Science Foundation of China (31822046, 31772355, and 31550110201), and the Henan University of Science and Technology (HAUST) Research Start-Up Fund for New Faculty (13480058).

REFERENCES

AbdElgawad, H., Farfan-Vignolo, E. R., de Vos, D., and Asard, H. (2015). Elevated CO(2) mitigates drought and temperature-induced oxidative stress differently in grasses and legumes. *Plant Sci.* 231, 1–10. doi: 10.1016/j.plantsci.2014.11.001

Ahammed, G. J., Li, X., Yu, J., and Shi, K. (2015). NPR1-dependent salicylic acid signaling is not involved in elevated CO2-induced heat stress tolerance in Arabidopsis thaliana. *Plant Signal Behav.* 10:e1011944. doi: 10.1080/15592324.2015.1011944

Ahuja, I., de Vos, R. C., Bones, A. M., and Hall, R. D. (2010). Plant molecular stress responses face climate change. *Trends Plant Sci.* 15, 664–674. doi: 10.1016/j.tplants.2010.08.002

Amthor, J. S. (1995). Terrestrial higher-plant response to increasing atmospheric [CO2] in relation to the global carbon cycle. *Global Change Biol.* 1, 243–274. doi: 10.1111/j.1365-2486.1995.tb00025.x

Brestic, M., Zivcak, M., Hauptvogel, P., Misheva, S., Kocheva, K., Yang, X., et al. (2018). Wheat plant selection for high yields entailed improvement of leaf anatomical and biochemical traits including tolerance to non-optimal temperature conditions. *Photosynth. Res.* 136, 245–255. doi: 10.1007/s11120-018-0486-z

Cassia, R., Nocioni, M., Correa-Aragunde, N., and Lamattina, L. (2018). Climate change and the impact of greenhouse gasses: CO2 and NO, friends and foes of plant oxidative stress. *Front. Plant Sci.* 9:273. doi: 10.3389/fpls.2018.00273

Cousins, A. B., Johnson, M., and Leakey, A. D. B. (2014). Photosynthesis and the environment. *Photosynth. Res.* 119, 1–2. doi: 10.1007/s11120-013-9958-3

Ethier, G. J., and Livingston, N. J. (2004). On the need to incorporate sensitivity to CO2 transfer conductance into the farquhar-von caemmerer-berry leaf photosynthesis model. *Plant Cell Environ.* 27, 137–153. doi: 10.1111/j.1365-3040.2004.01140.x

Farquhar, G. D., von Caemmerer, S., and Berry, J. A. (1980). A biochemical model of photosynthetic CO2 assimilation in leaves of C3 species. *Planta* 149, 78–90. doi: 10.1007/BF00386231

Field, C. B., Barros, V. R., Mach, K., and Mastrandrea, M. (2014). *Climate Change 2014: Impacts, Adaptation, and Vulnerability*. New York, NY: Cambridge University Press. doi: 10.1017/CBO9781107415379

Force, L., Critchley, C., and van Rensen, J. J. S. (2003). New fluorescence parameters for monitoring photosynthesis in plants. *Photosynth. Res.* 78:17. doi: 10.1023/A:1026012116709

Foyer, C. H. (2018). Reactive oxygen species, oxidative signaling and the regulation of photosynthesis. *Environ. Exp. Bot.* 154, 134–142. doi: 10.1016/j.envexpbot.2018.05.003

Jabs, T., Dietrich, R. A., and Dangl, J. L. (1996). Initiation of runaway cell death in an *Arabidopsis* mutant by extracellular superoxide. *Science* 273, 1853–1856. doi: 10.1126/science.273.5283.1853

Jayawardena, D. M., Heckathorn, S. A., Bista, D. R., Mishra, S., Boldt, J. K., and Krause, C. R. (2017). Elevated CO2 plus chronic warming reduce nitrogen uptake and levels or activities of nitrogen-uptake and -assimilatory proteins in tomato roots. *Physiol. Plant.* 159, 354–365. doi: 10.1111/ppl.12532

Kaur, H., Sirhindi, G., Bhardwaj, R., Alyemeni, M. N., Siddique, K. H. M., and Ahmad, P. (2018). 28-homobrassinolide regulates antioxidant enzyme activities and gene expression in response to salt- and temperature-induced oxidative stress in *Brassica juncea*. *Sci. Rep.* 8:8735. doi: 10.1038/s41598-018-27032-w

Klughammer, C., and Schreiber, U. (2008). Saturation pulse method for assessment of energy conversion in PSI. *PAM Appl. Notes* 1, 11–14.

Krall, J. P., and Edwards, G. E. (1992). Relationship between photosystem II activity and CO2 fixation in leaves. *Physiol. Plant* 86, 180–187. doi: 10.1111/j.1399-3054.1992.tb01328.x

Law, M. Y., Charles, S. A., and Halliwell, B. (1983). Glutathione and ascorbic acid in spinach (*Spinacia oleracea*) chloroplasts. The effect of hydrogen peroxide and of Paraquat. *Biochem. J.* 210, 899–903. doi: 10.1042/bj2100899

Lawlor, D. W., and Tezara, W. (2009). Causes of decreased photosynthetic rate and metabolic capacity in water-deficient leaf cells: a critical evaluation of mechanisms and integration of processes. *Ann. Bot.* 103, 561–579. doi: 10.1093/aob/mcn244

Li, H., Ahammed, G. J., Zhou, G., Xia, X., Zhou, J., Shi, K., et al. (2016). Unraveling main limiting sites of photosynthesis under below and above ground heat stress in cucumber and the alleviatory role of luffa rootstock. *Front. Plant Sci.* 7:746. doi: 10.3389/fpls.2016.00746

Li, X., Ahammed, G. J., Zhang, Y. Q., Zhang, G. Q., Sun, Z. H., Zhou, J., et al. (2015). Carbon dioxide enrichment alleviates heat stress by improving cellular redox homeostasis through an ABA-independent process in tomato plants. *Plant Biol.* 17, 81–89. doi: 10.1111/plb.12211

Ohama, N., Sato, H., Shinozaki, K., and Yamaguchi-Shinozaki, K. (2017). Transcriptional regulatory network of plant heat stress response. *Trends Plant Sci.* 22, 53–65. doi: 10.1016/j.tplants.2016.08.015

Pfündel, E., Klughammer, C., and Schreiber, U. (2008). Monitoring the effects of reduced PS II antenna size on quantum yields of photosystems I and II using the Dual-PAM-100 measuring system. *PAM Appl. Notes* 1, 21–24.

Raines, C. A. (2011). Increasing photosynthetic carbon assimilation in C3 plants to improve crop yield: current and future strategies. *Plant Physiol.* 155, 36–42. doi: 10.1104/pp.110.168559

Rao, M. V., Hale, B. A., and Ormrod, D. P. (1995). Amelioration of ozone-induced oxidative damage in wheat plants grown under high carbon dioxide (role of antioxidant enzymes). *Plant Physiol.* 109, 421–432. doi: 10.1104/pp.109.2.421

Rapacz, M. (2007). Chlorophyll a fluorescence transient during freezing and recovery in winter wheat. *Photosynthetica* 45, 409–418. doi: 10.1007/s11099-007-0069-2

Robredo, A., Pérez-López, U., Lacuesta, M., Mena-Petite, A., and Muñoz-Rueda, A. (2010). Influence of water stress on photosynthetic characteristics in barley plants under ambient and elevated CO2 concentrations. *Biol. Plant.* 54, 285–292. doi: 10.1007/s10535-010-0050-y

Sage, R. F., and Coleman, J. R. (2001). Effects of low atmospheric CO2 on plants: more than a thing of the past. *Trends Plant Sci.* 6, 18–24. doi: 10.1016/S1360-1385(00)01813-6

Strasser, B. J., and Strasser, R. J. (1995). "Measuring fast fluorescence transients to address environmental questions: the JIP-test," in *Photosynthesis: From Light*

to Biosphere, Vol. 5, ed. P. Mathis (Dordrecht: Kluwer Academic Publishers), 977–980.

Strasser, R., and Govindjee, G. (1992). *On The OJIP Fluorescence Transient in Leaves and d1 Mutants of Chlamydomonas-Reinhardtii, Photosynthesis Research*. Dordrecht: Kluwer Academic Publishers.

Strasser, R. J., Tsimilli-Michael, M., and Srivastava, A. (2004). *Analysis of the Chlorophyll a Fluorescence Transient*. Berlin: Springer. doi: 10.1007/978-1-4020-3218-9_12

Takahashi, S., and Murata, N. (2008). How do environmental stresses accelerate photoinhibition? *Trends Plant Sci.* 13, 178–182. doi: 10.1016/j.tplants.2008.01.005

Thordal-Christensen, H., Zhang, Z. G., Wei, Y. D., and Collinge, D. B. (1997). Subcellular localization of H2O2 in plants. H2O2 accumulation in papillae and hypersensitive response during the barley-powdery mildew interaction. *Plant J.* 11, 1187–1194. doi: 10.1046/j.1365-313X.1997.11061187.x

von Caemmerer, S., and Farquhar, G. D. (1981). Some relationships between the biochemistry of photosynthesis and the gas-exchange of leaves. *Planta* 153, 376–387. doi: 10.1007/BF00384257

Wang, F., Wu, N., Zhang, L., Ahammed, G. J., Chen, X., Xiang, X., et al. (2018). Light signaling-dependent regulation of photoinhibition and photoprotection in tomato. *Plant Physiol.* 176, 1311–1326. doi: 10.1104/pp.17.01143

Xu, Z., Jiang, Y., and Zhou, G. (2015). Response and adaptation of photosynthesis, respiration, and antioxidant systems to elevated CO2 with environmental stress in plants. *Front. Plant Sci.* 6:701. doi: 10.3389/fpls.2015.00701

Yamori, W., Sakata, N., Suzuki, Y., Shikanai, T., and Maniko, A. (2011). Cyclic electron flow around photosystem I via chloroplast NAD(P)H dehydrogenase (NDH) complex performs a significant physiological role during photosynthesis and plant growth at low temperature in rice. *Plant J.* 68, 966–976. doi: 10.1111/j.1365-313X.2011.04747.x

Yan, K., Chen, P., Shao, H., Shao, C., Zhao, S., and Brestic, M. (2013). Dissection of photosynthetic electron transport process in sweet sorghum under heat stress. *PLoS One* 8:e62100. doi: 10.1371/journal.pone.0062100

Yi, Z., Li, S., Liang, Y., Zhao, H., Hou, L., Yu, S., et al. (2018). Effects of exogenous spermidine and elevated CO_2 on physiological and biochemical changes in tomato plants under iso-osmotic salt stress. *J. Plant Growth Regul.* 37, 1222–1234. doi: 10.1007/s00344-018-9856-1

Yoshioka, M., Uchida, S., Mori, H., Komayama, K., Ohira, S., Morita, N., et al. (2006). Quality control of photosystem II - Cleavage of reaction center D1 protein in spinach thylakoids by FtsH protease under moderate heat stress. *J. Biol. Chem.* 281, 21660–21669. doi: 10.1074/jbc.M602896200

Zhang, T.-J., Feng, L., Tian, X.-S., Yang, C.-H., and Gao, J.-D. (2015). Use of chlorophyll fluorescence and P700 absorbance to rapidly detect glyphosate resistance in goosegrass (*Eleusine indica*). *J. Integr. Agric.* 14, 714–723. doi: 10.1016/S2095-3119(14)60869-8

Zhang, X., Hogy, P., Wu, X. N., Schmid, I., Wang, X., Schulze, W. X., et al. (2018). Physiological and proteomic evidence for the interactive effects of post-anthesis heat stress and elevated CO2 on wheat. *Proteomics* doi: 10.1002/pmic.201800262 [Epub ahead of print].

Zhao, Z., Hu, X., and Ross, C. W. (1987). Comparison of tissue preparation methods for assay of nicotinamide coenzymes. *Plant Physiol.* 84, 987–988. doi: 10.1104/pp.84.4.987

Zinta, G., Abdelgawad, H., Peshev, D., Weedon, J. T., Van Den Ende, W., Nijs, I., et al. (2018). Dynamics of metabolic responses to periods of combined heat and drought in *Arabidopsis thaliana* under ambient and elevated atmospheric CO2. *J. Exp. Bot.* 69, 2159–2170. doi: 10.1093/jxb/ery055

Conflict of Interest Statement: The authors declare that the research was conducted in the absence of any commercial or financial relationships that could be construed as a potential conflict of interest.